On the occurrence of a metastable tetragonal t'-phase in a ZrO_2–13.6 mole % MgO ceramic and its microscopic thermal evolution

M. C. Caracoche,[a] P. C. Rivas,[b] A. F. Pasquevich,[a] and A. R. López García[b]
Departamento de Física, UNLP, C. C. N° 67, 1900 La Plata, Argentina

E. Aglietti[b] and A. Scian[b]
Centro de Tecnología en Recursos Minerales y Cerámica, C. C. N° 49, 1897 M. B. Gonnet, Argentina

(Received 25 April 1991; accepted 5 November 1992)

The time-differential perturbed angular correlation technique has been used to investigate the thermal behavior of a ZrO_2–13.6 mole % MgO ceramic between room temperature and 1423 K. Two different quadrupole hyperfine interactions corresponding to a tetragonal structure have been found to result on cooling the ceramic from the single-phase cubic field. One of them agrees with that depicting the pure t–ZrO_2 tetragonal phase and the other one has been interpreted as describing a high-MgO-content nontransformable t'–ZrO_2 phase. As temperature increases, the latter gives rise to a similar but fluctuating interaction related to the oxygen vacancies mobility and which shows a thermal behavior analogous to that already reported for the stabilized cubic ZrO_2. Above 1100 K these dynamic t'-sites transform into pure tetragonal ones which behave ordinarily, suffering the $t \rightarrow m$ phase transition when cooling to room temperature. Differences found between TDPAC results and information drawn from other techniques are discussed.

I. INTRODUCTION

The investigation of high technology ceramics has led scientists to study zirconia,[1,2] with special interest in the modification of its properties by the addition of cubic-stabilizing oxides. In fact, it is known that if appropriate amounts of oxides as CaO, Y_2O_3, MgO, or rare earth oxides are added to zirconia, ceramics with optimum electrical and mechanical properties can be achieved. This process allows the stabilization at moderate temperatures of either the cubic or the tetragonal high-temperature crystallographic phases of zirconia (CZP or TZP), thus avoiding deleterious cracking which takes place at the tetragonal to monoclinic phase change on cooling, or otherwise, the intimate mixture of phases known as partially stabilized zirconia (PSZ), which leads to a significant improvement in toughness resulting from the stress-induced metastable tetragonal-monoclinic transformation. These solid solutions present a disordered fluorite-type structure in which the stabilizing cations and the concomitant oxygen vacancies are randomly distributed on regular sites of the anionic and cationic sublattices, respectively. Depending on temperature and the time scale of the technique employed, oxygen diffusion connected to ionic conductivity has been observed to occur.

The time-differential perturbed-angular-correlation (TDPAC) technique has proved to be highly efficient in investigating structural and electronic properties of solids via the determination of the hyperfine interaction between radioactive impurities and the extranuclear electric field gradients (EFG's) arising from nearby electrons and nuclei. Baudry *et al.*[3] have studied cubic ZrO_2–Y_2O_3 and ZrO_2–CaO ceramics by TDPAC between room temperature (RT) and 1423 K. Above 620 K they have found dynamic effects, having concluded that the observed asymmetric thermal behavior of the nuclear relaxation λ vs T^{-1} is consistent with a distribution of the activation energy controlling the local motion of oxygen vacancies. Jaeger *et al.*[4] and Gardner *et al.*[5] have also investigated zirconia/yttria alloys of different compositions using the same technique. In both stabilized high temperature phases obtained, cubic or tetragonal depending on composition, they have observed some experimental evidence of the atomic diffusion. In a sample where the tetragonal phase was expected above 500 K,[4] the spectrometer resolution did not allow the authors to resolve the low-temperature spectra. At higher temperatures, on the other hand, the contribution of rapidly diffusing oxygen vacancies gave a small and relatively uniform EFG. In cubic samples,[5] instead, at intermediate temperatures where oxygen vacancy jump times became comparable with the TDPAC coupling frequencies, an accurate experimental determination of the relaxation constant could be carried out. These data

[a]Researcher for CICPBA–Argentina.
[b]Researcher for CONICET–Argentina.

led, for temperatures above 1000 K, to an activation energy in reasonable agreement with that reported for the ionic conduction.

In the present work, a TDPAC experiment on a ZrO_2–13.6 mole% MgO ceramic was carried out between RT and 1416 K. The results are discussed on the basis of data of phase equilibria conditions and zirconia polymorphism.

II. EXPERIMENTAL

The TDPAC technique measures the perturbation in the angular distribution of nuclear radiation in cascade due to the interaction between the radioactive probe nucleus and its surroundings. When a nucleus emits radiations γ_1 and γ_2 in cascade, separated by a time t, the probability that the emission directions form a θ angle is given by the angular function $W(\theta, t)$ which can be briefly written as[6]:

$$W(\theta,t) = 1 + A_2G_2(t)P_2(\cos\ \theta) + A_4G_4(t)P_4(\cos\ \theta) \quad (1)$$

where A_2 and A_4 are coefficients that depend on the spin involved in the transitions as well as of the radiation multipolarities, $P_2(\cos\ \theta)$ and $P_4(\cos\ \theta)$ are the Legendre polynomials, and $G_2(t)$ and $G_4(t)$ are the perturbation factors which describe the nucleus-surroundings hyperfine interaction and inform about the EFG. In the frame of the principal axes, this EFG is usually characterized through its major component V_{zz} and the asymmetry parameter defined by $\eta = (V_{xx} - V_{yy})/V_{zz}$ which varies from zero for axially asymmetric sites to unity for maximally nonsymmetric sites. The ordinary hafnium impurities in zirconium (about 3%) allowed us to employ the TDPAC technique for this investigation. ^{181}Hf activity was obtained by neutron irradiation at the Comisión Nacional de Energía Atómica, Argentina, and gave rise, by β^- decay, to the efficient 133–482 keV γ-γ cascade of ^{181}Ta with an intermediate level of spin $I = 5/2$ and a quadrupole moment $Q = 2.53$ barns used in this work as the nuclear probe. Indeed, if the Q value is large enough, the probe nuclei are sensitive to the EFG's generated by the peculiar charge distribution of the environments at zirconium sites, and the resulting perturbation of the angular correlation constitutes a measurable magnitude. As the involved cascade exhibits $A_4 < A_2$, we have focused the interest of our measurements in the $R(t) \equiv A_2G_2(t)$ factor exclusively. For a static quadrupole interaction in a polycrystalline sample, the perturbation factor has the form[6]:

$$G_2^s(t) = \sigma_{20} + \sum_{n=1}^{3} \sigma_{2n} e^{-\delta\omega_n t} \cos(\omega_n t) \quad (2)$$

where the superscript s denotes the static character of the interaction, $\sigma_{20}(\eta)$ and $\sigma_{2n}(\eta)$ have known functional dependence, ω_n are functions of η and of the quadrupole frequency $\omega_Q = eQV_{zz}/[4I(2I - I)h]$, and δ is a Lorentzian frequency width related to the existence of imperfections or impurities in the lattice. In the presence of a fluctuating EFG, the perturbation factor results damped with time and the simple expression:

$$G_2^d(t) = e^{-\lambda t} G_2^s(t) \quad (3)$$

is frequently used for fitting the experimental data.[3] To consider the possibility of several crystalline surroundings of the probe nuclei, each one of relative abundance f_i, a superposition of perturbation factors weighted with f_i must be assumed. The sample of ZrO_2 used in this work was prepared by precipitating a zirconium chloride oxide plus a magnesium chloride solution, by addition of a predetermined amount of NH_4OH (1 : 1). The solution was stirred very quickly and the precipitate was filtered. The collected material was then washed by repeated cycles with distilled water until a negative test for Cl^- was achieved. The sample was dried in air at 383 K and the as-prepared powder was calcinated at 1373 K and then pressed at 2500 kg/cm^2 to form pellets. Finally, these were fired at 1923 K for 50 min and furnace cooled, reaching to 1100 K in 1 h.

In order to identify the phases present in the as-prepared sample, an x-ray powder diffraction analysis over the regions $2\theta = 27°$–$32°$ and $72°$–$76°$ and a Raman spectrum between 200 cm^{-1} and 800 cm^{-1} were performed. The thermal stability of the sample was analyzed up to 1573 K by means of differential thermal analysis (DTA) in undried air, at atmospheric pressure, and at the rate of 10 K/min. TDPAC spectra were taken at increasing temperatures, and at intervals of approximately 50 K. Each measurement lasted at least one day. To investigate the effects of the cumulative thermal treatments on the stability of the sample, some coolings to RT were carried out between measurements.

III. RESULTS AND DISCUSSION

According to the phase diagram shown in Fig. 1,[1] the ZrO_2–13 mole% MgO alloy prepared would have had cubic symmetry. The x-ray powder diagram in the region of low angles did not provide distinction between the cubic and tetragonal phases of ZrO_2. In the region of high angles, instead, it led to the suspicion that the phase obtained presented tetragonal symmetry. As is already shown,[7–9] the cubic peak in this region appears near $2\theta = 73.7°$, between the positions of the two tetragonal peaks at around 74.4° and 73°. Our diffraction spectrum showed only one peak, but at 74.5° coincident with the most intense tetragonal diffraction peak. The Raman spectrum (see Fig. 2) revealed undoubtedly that

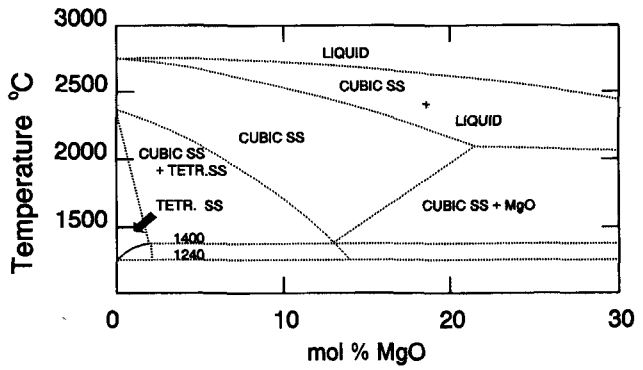

FIG. 1. ZrO_2–MgO phase diagram.[1]

the phase achieved after cooling had predominantly tetragonal structure. In fact, the four bands expected for this phase over 200 cm^{-1} can be clearly observed.[10] In addition, there is no evidence either of the typical single band around 500 cm^{-1} predicted for the fluorite-type cubic phase[11] or of some similitude between our spectrum and those determined for the cubic phases in the Y_2O_3–Zr_2 and CaO–ZrO_2 systems, which show strong polarized extended Raman patterns and only a broad peak near 600 cm^{-1}.[12–14] Regarding DTA results, the absence of peaks indicated the thermal stability of the fabricated zirconia.

In Fig. 3 representative TDPAC spectra taken at selected temperatures and also their corresponding Fourier transforms are plotted. Figure 4 shows the thermal evolution of the fitted quadrupole parameters of the interactions found over the whole thermal range investigated, excluding those already known of the monoclinic phase.

At RT two interactions were present: the less populated one (14%) of quadrupole parameters corresponding to the intense, axially symmetric and monochromatic EFG of the t-high temperature tetragonal phase[4,15] [(●) in Fig. 4], and another one, denoted by t'–ZrO_2 hereinafter, which is characterized by an EFG of lower quadrupole frequency and relevant asymmetry parameter and frequency distribution width [(▲) in Fig. 4]. This situation did not change up to 605 K, above which temperature a third contribution to the hyperfine interaction corresponding to a fluctuating EFG with perturbation factor as that described by Eq. (3) had to be added to get a satisfactory fit [(■) in Fig. 4]. The new interaction grew at the expense of t' and presented not very different quadrupole frequency and asymmetry parameters, the distinguishing feature being its dynamic nature. These evidences led us to visualize these two competitive interactions as arising from the same zirconium environments and to infer that oxygen vacancy diffusion already known to take place in this thermal region in stabilized zirconias[3–5] became thermally activated. The observed gradual change from static into dynamic t'-sites went to completion at 963 K. The somewhat lower quadrupole

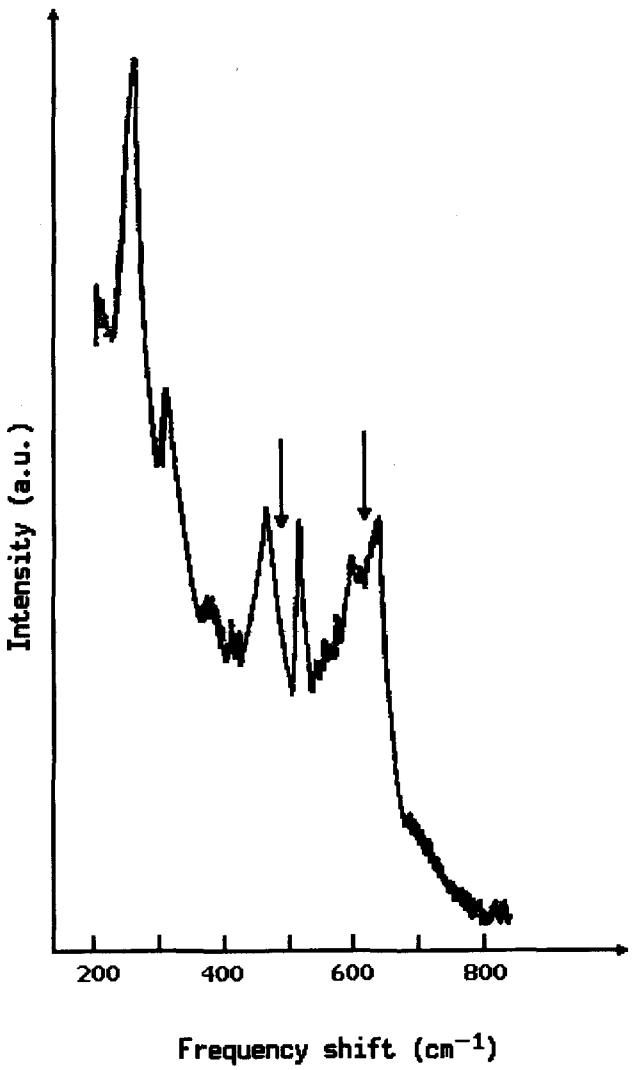

FIG. 2. Raman spectrum of the as-prepared ZrO_2–13.6 mole% MgO ceramic. The band at 520 cm^{-1} is due to the plasma line from the laser oscillation source. The characteristic tetragonal band at 270 cm^{-1} is clearly the most intense one. The arrows indicate the frequency shifts reported for the cubic phase (see text).

frequency of the fluctuating EFG relative to that of the static one can be understood in terms of the oxygen vacancy thermal averaging.

In Fig. 5 the thermal evolution of the involved relaxation constant λ vs T^{-1} in the range 743 K–1343 K is plotted. Though the characteristic asymmetric behavior already found by other authors in stabilized c–ZrO_2[3,5] can be clearly observed, our data were not sufficient to deduce a reliable activation energy. Up to 1030 K the λ increase with temperature can be related to a slow fluctuation of the EFG since the relaxation constant must in this case be proportional to the inverse of the correlation time of the oxygen vacancy jumps. At higher temperatures, on the other hand, λ decreased with increasing temperatures, evidencing a fast relaxation regime with an estimated activation energy somewhat lower than those

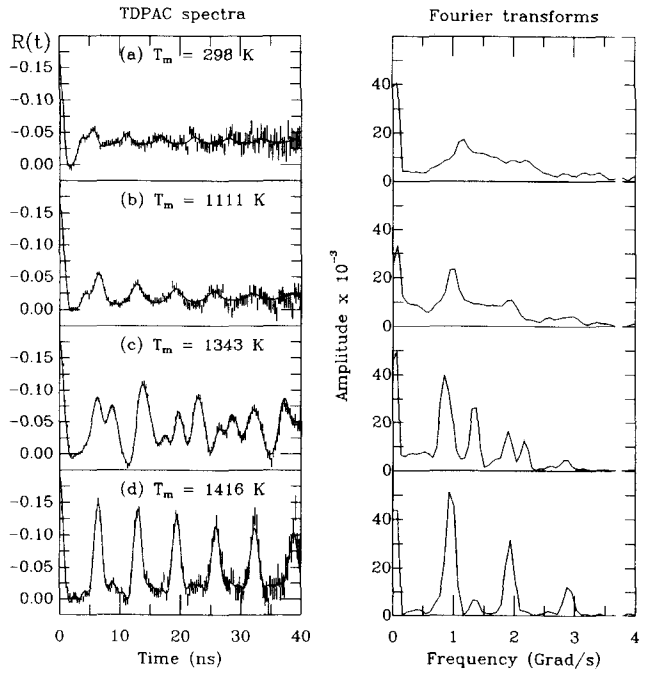

FIG. 3. Relevant TDPAC spectra and their corresponding Fourier transforms. The solid curves on the time spectra are the best computer fits. T_m = (a) 298 K, (b) 1111 K, (c) 1343 K, and (d) 1416 K.

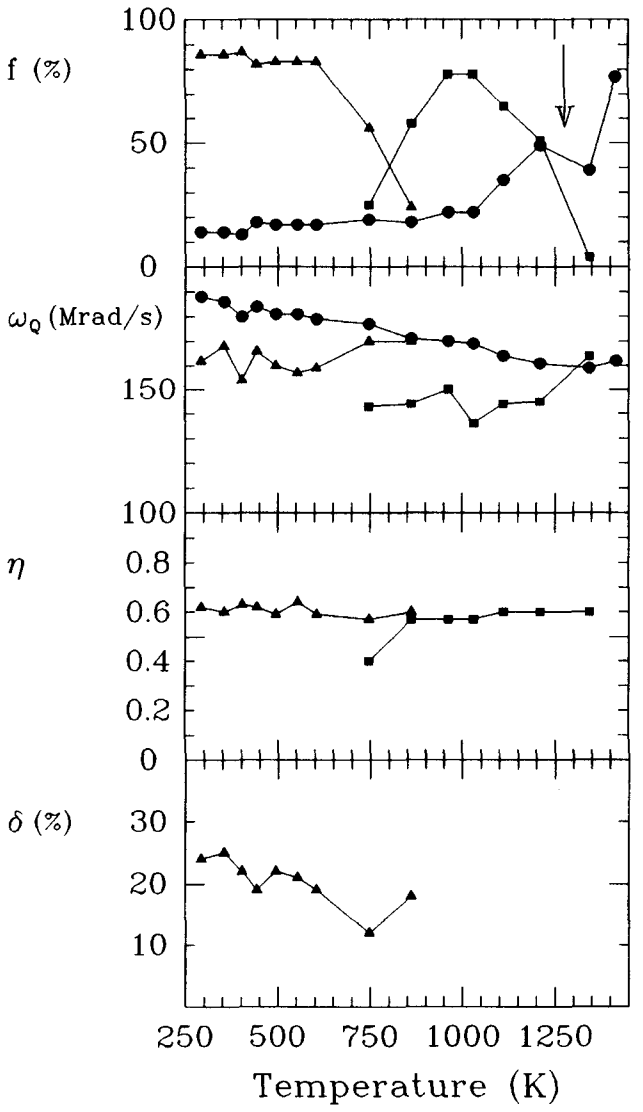

FIG. 4. Thermal evolution of the relative fractions and quadrupole parameters fitted to the hyperfine interactions found over the whole thermal range investigated. (●) t–ZrO_2, (▲) static t'–ZrO_2, and (■) dynamic t'–ZrO_2. Monoclinic zirconia existing at the two highest temperatures has not been included. In all cases the errors are negligible. Solid lines drawn are just to guide the eye.

determined elsewhere for some cubic zirconias. Simultaneously, a clear growth of the population of the t-phase at the expense of dynamic t'-sites took place. Though several previous cooling treatments to RT performed between measurements at increasing temperatures seemed not to alter the monotonous evolution of the hyperfine interaction, the one performed between 1200 K and 1343 K (denoted by an arrow in Fig. 4) produced a dramatic effect, as was inferred from the TDPAC result obtained at 1343 K. In fact, the mixture of monoclinic (57%) and tetragonal t-sites (39%) fitted at this temperature revealing that the ordinary $m \rightarrow t$ phase transformation was occurring, evidenced that the inverse $t \rightarrow m$ transformation had taken place during the previous cooling to RT. At the highest temperature of 1416 K, the structural change had progressed up to 77% of tetragonal phase. A final RT measurement led to m–ZrO_2, though showing some degree of distortion (frequency distribution width of 7%).

The experimental results reported above can be interpreted as follows:

(i) From Raman and TDPAC results, it can be inferred that two different structures of tetragonal symmetry are present upon cooling to RT the specimen sintered at 1923 K for 50 min. From the inspection of their quadrupole parameters, these phases can be thought to correspond to zero-MgO and high-MgO contents in tetragonal zirconium neighborhoods, respectively. In fact, while the first of them presents a hyperfine interaction identical to that of the pure tetragonal high-temperature phase, the second one shows relevant asymmetry parameter and frequency spread which can be assigned to the tetragonal zirconium environments greatly distorted and disordered by oxygen vacancies and/or dopant cations. Following previous usage[16] this high-MgO form has been denoted by t'–ZrO_2. The $c \rightarrow t'$ transformation, reported as diffusionless and displacive, was observed to appear in ZrO_2–Y_2O_3 alloys of appropriate composition when, starting from the single phase c–ZrO_2, the sample was quenched to avoid the occurrence of the diffusional phase transformation $c \rightarrow t$ upon passing through the $c + t$ field.[16–18] The thermodynamic and structural conditions which define it

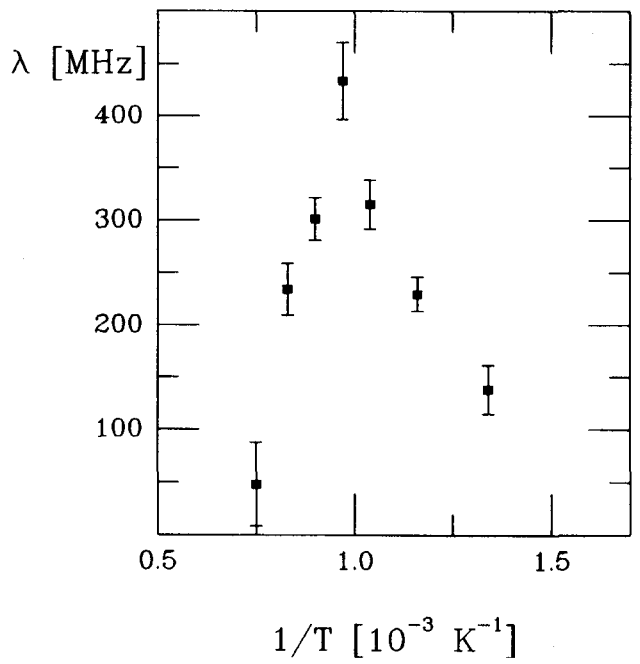

FIG. 5. Relaxation constant versus reciprocal temperature.

allowed explanation of the coexistence of three different twin variants of t'–ZrO_2 form whose c-axes are nearly parallel to either the X, Y, or Z axis of the cubic matrix. Within each twin, a domain structure arising because of the lowering of symmetry during the transformation is present, characterized by antiphase boundaries (APB's) evidenced by TEM. Also, this resulting composition-invariant high-solute-content phase is much more resistant to the martensitic transformation to monoclinic symmetry than is t–ZrO_2 and has hence been called "nontransformable". The above interpretation of our results leads to the assumption that the t'–ZrO_2 form could exist also for some compositions of the ZrO_2–MgO alloy, e.g., the ZrO_2–13.6 mole% MgO ceramic under investigation. As in our case the cooling to RT did not involve the passage through the $c + t$ field (see Fig. 1), the quenching condition for its occurrence became unnecessary. At this point, it is worth mentioning that Knapp *et al.*,[19] investigating a Mg–PSZ ceramic by SEM and other techniques, have observed a fine-grained feature intermediate between large grains and fine precipitates and which showed the characteristic twinning of monoclinic zirconia. Since the large grains showed the expected higher MgO content predicted for cubic zirconia while the fine precipitates showed the much lower content corresponding to tetragonal zirconia and XRD revealed no monoclinic phase present in the sample, the authors believe that this phase of intermediate MgO content could be a tetragonal one other than the precipitate phase, similar to that produced in Y_2O_3–ZrO_2 TZP's and not yet reported in the literature for MgO–ZrO_2 PSZ.

The presence of the accompanying 14% of t–ZrO_2 phase in the initial TDPAC measurement deserves a special discussion. According to the phase diagram, it does not seem possible that the t-phase had been produced via the $c \rightarrow t$ diffusional transformation,[18] but instead that it had stabilized at high temperature along with the cubic phase due to insufficient sintering conditions for the stabilization of the latter exclusively. Upon cooling to RT, while the c–ZrO_2 phase underwent the displacive and diffusionless transformation to t'–ZrO_2, the t-fraction remained unaffected without reverting to the monoclinic phase, perhaps due either to a very small grain size[20] and/or to the fact of its existence as mere precipitates inside the highly predominant constraining t'-matrix.

(ii) The hardness in distinguishing between the cubic and the tetragonal forms in the x-ray powder diagram may be due to a very low tetragonality ($c/a \approx 1$) of the t'–ZrO_2 which depends, as is known for Y–PSZ, on the stabilizing oxide content in the alloy investigated.[16]

(iii) The static t'-sites transformation into dynamic ones above 605 K can be explained in terms of the oxygen vacancies mobility; if thermally activated oxygen vacancies diffusion occurs, most likely only zirconium neighborhoods containing doping effects will experience a fluctuating EFG involving nuclear relaxation rates varying with temperature. Concerning the asymmetry observed in the λ vs T^{-1} plot of Fig. 5, Jaeger *et al.*[21] have demonstrated that it results from a spatial averaging of vacancy interactions.

(iv) Up to 1100 K, the t'-form remains unaltered upon heating or cooling, thus confirming its "nontransformable" character. The changes observed by TDPAC at higher temperatures, e.g., the $t' \rightarrow t$ transformation with increasing temperatures and the subsequent $t \rightarrow m$ phase transformation that must have taken place upon cooling from 1200 K to RT, can be explained as follows: as the thermal range of stability of the ordinary tetragonal phase was approached, t'-sites began to segregate their MgO content and gradually converted into the pure tetragonal form. This situation, added to the fact that tetragonal grains had probably grown during the long annealings of each measurement at increasing temperatures, made the bulk $t \rightarrow m$ transition possible when cooling to RT. The present hypothesis is coherent with the knowledge of the insolubility of MgO in the monoclinic phase observed in the phase diagram of Fig. 1 and with the reported instability of PSZ's, which have a maximum long-term application temperature of 1173 K.[22] Neither of the two changes reported above were revealed by the DTA performed at a constant rate of 10 K/min. While the first of them might involve no transformation energy, and hence would not be observed in the heating thermal curve, the second one would have to appear as an exothermic peak on the cooling curve. This

discrepancy can be understood only on the hypothesis that the completely different thermal treatments suffered by the ceramic under study in both experiments, TDPAC and DTA, resulted in a different ability to retain the stabilization achieved originally.

IV. CONCLUSIONS

(1) Proper MgO content and a time of 50 min at a sintering temperature of 1923 K have proven to be insufficient to obtain the cubic stabilized phase of zirconia.

(2) Most zirconium sites exhibited surroundings with high MgO content, which might be assigned to a nontransformable tetragonal t'–ZrO_2 phase not reported in the ZrO_2–MgO phase diagram.

(3) Above 700 K, t'–ZrO_2 sites showed a thermally activated movement of similar characteristics to that reported for the cubic phase and attributed to oxygen vacancies diffusion.

(4) Changes occurring above 1100 K by TDPAC and not revealed by the DTA suggest that the retention of the stability achieved on preparation was dependent on the subsequent thermal treatments suffered by the sample.

(5) The main results reported in this paper—the metastability of the pretended cubic phase and the dependence of the stability of the tetragonal structures obtained on the subsequent heating treatments—have led the authors to fabricate Mg–PSZ ceramics varying (a) the preparation method, (b) the MgO content, and (c) the cooling rate from the sintering temperature. The TDPAC investigation of these powders is in progress.

ACKNOWLEDGMENTS

This work was partially supported by CONICET and CICPBA (Argentina). The authors are much indebted to Dra. E. B. Halac, from the Comisión Nacional de Energía Atómica, who supplied the Raman spectrum.

REFERENCES

1. R. Stevens, *Zirconia and Zirconia Ceramics* (Magnesium Elektron Ltd., U.K., 1986), and references therein.
2. Adv. Ceram., **24A** and **24B**: *Science and Technology of Zirconia III*, edited by Shigeyuki Sōmiya, Noborn Yamamoto, and Hiroaki Yanagida (The American Ceramic Society, Inc., Westerville, OH, 1988).
3. A. Baudry, P. Boyer, and A. L. de Oliveira, Hyp. Int. **10**, 1003 (1981).
4. H. Jaeger, J. Gardner, J. Haygarth, and R. L. Rasera, J. Am. Ceram. Soc. **69**, 458 (1986).
5. J. Gardner, H. Jaeger, H. T. Su, W. H. Warnes, and J. Haygarth, Physica B **150**, 223 (1988).
6. H. Frauenfelder and R. M. Steffen, in Alpha-, Beta-, and Gamma-Ray Spectroscopy, edited by K. Siegbahn (North-Holland, Amsterdam, 1965), p. 997.
7. K. Hishinuma, T. Kumaki, Z. Nakai, M. Yoshimura, and S. Sōmiya, Adv. Ceram. **24A**, 205 (1988).
8. T. Noma, M. Yoshimura, S. Sōmiya, M. Kato, M. Shibata, and H. Seto, Adv. Ceram. **24A**, 379 (1988).
9. P. Morrell and R. Taylor, Adv. Ceram. **24B**, 932, 935 (1988).
10. R. Srinivasan, M. B. Harris, S. F. Simpson, R. J. De Angelis, and B. H. Davis, J. Mater. Res. **3**, 787 (1988).
11. C. M. Phillippi and K. S. Mazdiyasni, J. Am. Ceram. Soc. **54**, 254 (1971).
12. V. I. Aleksandrov, Yu. K. Voron'ko, B. V. Ignat'ev, E. E. Lomonova, V. V. Osiko, and A. A. Sobol', Sov. Phys. Solid State **20**, 305 (1978).
13. A. Feinberg and C. H. Perry, J. Phys. Chem. Solids **42**, 513 (1981).
14. V. G. Kerenidas and W. B. White, J. Phys. Chem. Solids **34**, 1873 (1973).
15. M. C. Caracoche, M. T. Dova, A. R. López García, J. A. Martínez, and P. C. Rivas, Hyp. Int. **39**, 117 (1988).
16. V. Lanteri, R. Chaim, and A. H. Heuer, J. Am. Ceram. Soc. **69**, C-258 (1986).
17. R. Chaim, M. Rühle, and A. H. Heuer, J. Am. Ceram. Soc. **68**, 427 (1985).
18. A. H. Heuer, R. Chaim, and V. Lanteri, Acta Metall. **35**, 661 (1987).
19. C. E. Knapp, K. E. Manwiller, and D. B. Arvidson, Adv. Ceram. **24A**, 369 (1988).
20. T. Sato and M. Shimada, J. Mater. Sci. **20**, 3988 (1985).
21. H. Jaeger, J. A. Gardner, R. L. Rasera, and W. E. Evenson, Bull. Am. Phys. Soc. **32**, 414 (1987).
22. U. Dworak, H. Olapinski, and W. Burger, Adv. Ceram. **24A**, 545 (1988).